

Twisted Heating-Cooling Transition of Near-field Radiation in Drifted Metasurfaces

Jiebin Peng,^{1,2,*} Zi Wang,¹ and Jie Ren^{1,†}

¹Center for Phononics and Thermal Energy Science, China-EU Joint Lab on Nanophononics, Shanghai Key Laboratory of Special Artificial Microstructure Materials and Technology, School of Physics Science and Engineering, Tongji University, 200092 Shanghai, China

²School of Physics and Optoelectronic Engineering, Guangdong University of Technology, Guangzhou 510006, Guangdong Province, PR China

The magic angle twisted bilayer systems give rise to many exotic phenomena in two-dimensional electronic or photonic platforms. Here, we study the twisted near-field energy radiation between graphene metasurfaces with nonequilibrium drifted Dirac electrons. Anomalous, we find unconventional radiative flux that directs heat from cold to hot. This far-from-equilibrium phenomenon leads to a heating-cooling transition beyond a thermal magic twist angle, facilitated by twist-induced photonic topological transitions. The underlying mechanism is related to the spectrum match and mismatch caused by the cooperation between the non-reciprocal nature of drifted plasmon polaritons and their topological features. Furthermore, we report the unintuitive distance dependence of radiative energy flux under large twist angles. The near-field radiation becomes thermal insulating when increasing to a critical distance, and subsequently reverses the radiative flux to increase the cooling power as the distance increases further. Our results indicate the promising future of nonequilibrium drifted and twisted devices and pave the way towards tunable radiative thermal management.

The manipulation of thermal-photon carrier density in the near-field has been extensively studied for many technological applications, including enhanced radiative cooling[1, 2], thermophotovoltaic[3, 4], and near-field imaging[5]. Inspired by the concept of magic-angle twisted bilayer graphene[6, 7], a magic-angle twisted photonic hyperbolic metasurface, such as a periodic array of graphene ribbons[8, 9], can be used to break the geometric symmetry and induce a topological transition in the isofrequency dispersion to control the photon carrier density[10]. Additionally, there are similar methods to control near-field heat transfer, such as anisotropic and gain thermal magnetoresistance[11, 12], twist-induced radiative thermal switches[13–17], and twisted thermophotovoltaic systems[18]. However, most twisted methods are carried out with passive systems and rely on the local equilibrium approximation, which is ultimately limited by the temperature bias that restricts the direction of energy flow always from hot to cold.

Recently, various methods have been explored to overcome the limitations of temperature bias and achieve active cooling effects. These methods include spatiotemporal modulation of the material permittivity[19, 20], rotation of the nanostructures[21], and regulation of photonic chemical potential[22–24] or current-biased graphene[25]. Owing to nonequilibrium nature of current-biased graphene, the distribution of radiation photons in current-biased graphene metasurface follows a fluid-like behavior, exhibiting non-reciprocity with time-reversal symmetry breaking[26–28]. The non-reciprocal hyperbolic plasmon polaritons in current-biased graphene metasurface thus emerge as an ideal platform for exploring the possibilities of twist-tunable heating-cooling transitions, resulting in a thermal magic angle.

In this Letter, we study the near-field radiative energy transfer between two hyperbolic graphene metasurfaces, with a focus on breaking both time-reversal and geometric symmetry. Specifically, we apply nonequilibrium drift current and twist

to one of the graphene metasurfaces and explore the cooperative interplay between the non-reciprocal nature of drifted plasmon polaritons and the twist-induced topological transition. Our findings reveal the presence of a transition angle between heating and cooling, as well as cooling flux beyond the magic twist angle. Notably, we observe an anomalous distance effect for large twist angles, which originates from the distinct distance dependencies of the heating and cooling modes. These results advance our understanding of near-field energy radiation and would have implications for the future development of thermal management.

Near-field radiative energy transfer.—We consider near-field radiative energy transfer between passive- and active-graphene metasurface with temperature differences $T_{1(2)}$ and twist angle θ [See Fig. 1(a)]. The bottom graphene layer is a passive layer without drift electrons ($v_1 = 0$) and the top graphene layer is an active layer with drift electrons ($v_2 = v_d$) in our calculation. A Cartesian coordinate system xyz ($x'y'z'$) is defined at the bottom (top) layer and the y (y') axis is along the direction of drift electron velocity. The twist angle θ is defined as the angle between the y' and y axis. From fluctuational electrodynamics[29, 30], the radiative energy flux can be expressed as

$$H = \int_0^\infty \frac{d\omega}{2\pi} \int_{-\infty}^\infty \frac{d\mathbf{k}}{4\pi^2} \hbar\omega(n_2 - n_1)\mathcal{Z}(v_d, \theta), \quad (1)$$

where $\mathbf{k} = [k_x, k_y]$ is the in-plane wave vector. $n_{1(2)} = 1/[e^{\hbar(\omega - k_y v_{1(2)})/k_b T_{1(2)}} - 1]$ is the drift Bose distribution with drift velocity $v_{1(2)}$ in y direction and $T_{1(2)}$ is temperature of bottom(top) layer[22, 31, 32]. For convenience, we define the energy transmission function of the energy flux in Eq. 1 as:

$$\mathcal{F}(\omega, k_x, k_y) = \hbar\omega(n_2 - n_1)\mathcal{Z}(v_d, \theta). \quad (2)$$

The energy flux spectrum $h(\omega)$ is integrand function of H in frequency space, i.e., $H = \int_0^\infty h(\omega)d\omega/2\pi$. The properties of energy transmission function in $\omega - k_y$ panel ($\mathcal{F}_{\omega k_y}$)

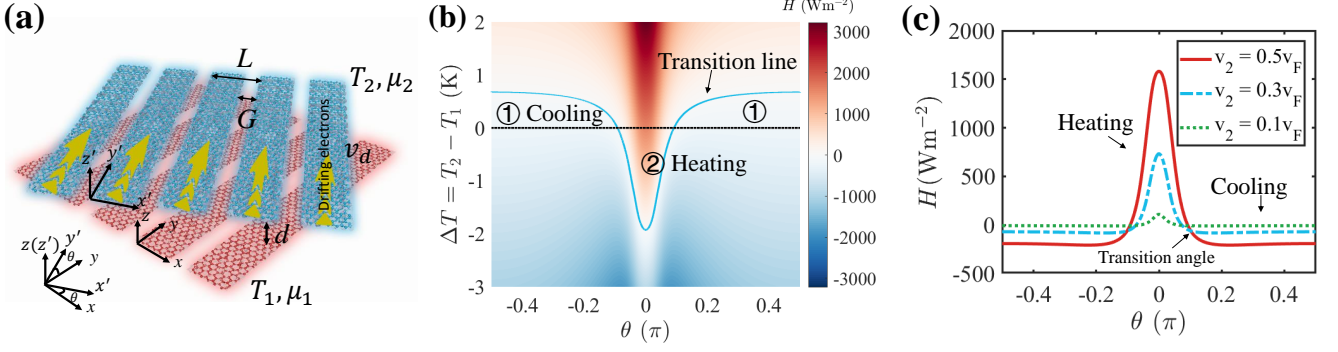


FIG. 1. (a) A schematic setup for twisted and drifted radiative energy transfer between two graphene metasurfaces with a gap separation d . The top layer is driven with an external voltage and has drifted electrons with constant velocity v_d . y' is defined as the direction of drift velocity in the top layer and tunable twist angle θ is defined as the anticlockwise rotation of y' with respect to y axis of the bottom layer. The chemical potentials of two layers are equal ($\mu_1 = \mu_2 = 0.1\text{eV}$). (b) Color plot for the energy flux as a function of twist angle θ and temperature bias $\Delta T = T_2 - T_1$ with fixed T_1 . The blue-solid line is the transition line with zero energy flux. (c) Energy flux as a function of twist angle θ with different drift velocities in zero temperature bias condition ($\Delta T = 0$). The magic angle is defined as the transition angle between positive and negative energy flux. v_F is the fermi velocity of graphene. The gap separation d is 100 nm and $T_1 = 300\text{K}$.

can be described by the function of \mathcal{F} after integrating k_x , i.e., $\mathcal{F}_{\omega k_y} = \int \mathcal{F} dk_x$. The energy transmission coefficient $\mathcal{Z}(\omega, k_x, k_y)$ with twist angle θ reads

$$\mathcal{Z} = \begin{cases} \text{Tr}[(\mathbf{I} - \mathbf{R}_2^\dagger \mathbf{R}_2) \mathbf{D} (\mathbf{I} - \mathbf{R}_1 \mathbf{R}_1^\dagger) \mathbf{D}^\dagger], & |\mathbf{k}| < k_0, \\ \text{Tr}[(\mathbf{R}_2^\dagger - \mathbf{R}_2) \mathbf{D} (\mathbf{R}_1 - \mathbf{R}_1^\dagger) \mathbf{D}^\dagger] e^{-2|k_z|d}, & |\mathbf{k}| > k_0, \end{cases} \quad (3)$$

where $k_0 = \omega/c$ is the wave vector in vacuum, c is light velocity in vacuum and $k_z = \sqrt{(\omega/c)^2 - \mathbf{k}^2}$ is the in(out)-of-plane wave vector in vacuum. \mathbf{I} denotes the identity matrix. The Fabry-Perot-like denominator matrix is written as $\mathbf{D} = (\mathbf{I} - \mathbf{R}_1 \mathbf{R}_2 e^{2ik_z d})^{-1}$. $\mathbf{R}_{1(2)}$ is the reflection coefficient matrix and related to the optical conductivity tensor of the bottom(top) metasurface.

Twisted optical conductivity tensor of the graphene metasurface with drift electrons.— Without loss of generality, we take the example of graphene metasurface. The graphene strip periodicity has width L and the air gap G is the separation distance between the neighboring graphene strips. The deeply subwavelength periodicity assumption is satisfied in our calculation, i.e., $L = 10\text{nm} \ll \lambda_{tm}$ (where λ_{tm} is the room temperature thermal wavelength). So that optical conductivity tensor $\bar{\sigma}^{\text{eff}} = [\sigma_{xx}^{\text{eff}}, \sigma_{xy}^{\text{eff}}, \sigma_{yx}^{\text{eff}}, \sigma_{yy}^{\text{eff}}]$ of graphene metasurface can be characterized with the effective medium theory[33]:

$$\begin{aligned} \sigma_{xx}^{\text{eff}} &= \frac{L\sigma_{xx}^g \sigma_{xx}^C}{W\sigma_{xx}^C + (L-W)\sigma_{xx}^g}, \quad \sigma_{xy(yx)}^{\text{eff}} = \sigma_{xx}^{\text{eff}} \frac{W\sigma_{xy}^g}{L\sigma_{xx}^g}, \\ \sigma_{yy}^{\text{eff}} &= \frac{W}{L}\sigma_{yy}^g - \frac{W\sigma_{yx}^g \sigma_{xy}^g}{L\sigma_{xx}^g} + \frac{\sigma_{yx}^{\text{eff}} \sigma_{xy}^{\text{eff}}}{\sigma_{xx}^{\text{eff}}}, \end{aligned} \quad (4)$$

where $\sigma_{xx}^C = -i\frac{\omega\epsilon_0 L}{\pi} \text{In} \left[\csc \left(\frac{\pi}{2} \frac{L-W}{L} \right) \right]$ is the nonlocal correction parameter taking into account the near-field coupling of adjacent ribbons. $\bar{\sigma}^g = [\sigma_{xx}^g, \sigma_{xy}^g; \sigma_{yx}^g, \sigma_{yy}^g]$ is the nonlocal optical conductivity tensor of graphene [34]. Furthermore,

we use a Doppler shift model [26] to study the drift effects of the metasurface in y direction:

$$\bar{\sigma}_d(\omega, v_d) \approx \frac{\omega}{\omega - k_y v_d} \bar{\sigma}_{\text{eff}}(\omega - k_y v_d). \quad (5)$$

The optical properties of graphene metasurface are anisotropic and the corresponding surface plasmon-polaritons becomes non-reciprocal due to the drifted electrons along the strips. The general formula for the optical conductivity tensor in k_x - k_y space with twist angle θ can be written as[35]:

$$\bar{\sigma}(\theta) = \mathcal{R}(\theta) \frac{1}{k_\rho} \begin{bmatrix} k_x & -k_y \\ k_y & k_x \end{bmatrix} \bar{\sigma}_d \frac{1}{k_\rho} \begin{bmatrix} k_x & k_y \\ -k_y & k_x \end{bmatrix} \mathcal{R}^{-1}(\theta), \quad (6)$$

where $\mathcal{R}(\theta)$ is the 2D rotation matrix and the positive θ corresponds to anticlockwise rotation of the top active graphene metasurface.

During the numerical calculation, the temperature of bottom passive layer T_1 is fixed at room temperature ($\sim 300\text{K}$). The chemical potentials of two layers are equal ($\sim 0.1\text{eV}$). The strip periodicity L for graphene metasurface is set as 10 nm and the air gap G is set as 5 nm. The relaxation time of graphene is $3.6 \times 10^{-13}\text{s}$ and the Fermi velocity v_F takes 10^6ms^{-1} . The cut-off wave vector in the \mathbf{k} -integration is set as $500k_0$.

Thermal magic twist angle of heating-cooling transition.— Fig. 1(b) shows the energy flux as a function of twist angle θ ranging from -0.5π to 0.5π and temperature bias $\Delta T = T_2 - T_1$ with fixed $T_1 = 300\text{K}$. We observe the active heating and cooling behaviors in $(\theta - \Delta T)$ phase diagram, that is the positive energy flux against the temperature gradient. The heating region ② is found to be close to zero twist angle, where the active-cold layer 2 can counterintuitively transfer energy into the passive-hot layer 1. By rotating the active layer beyond the transition twist angle ($\approx \pm 0.1\pi$), we can transform from the heating region ② into the cooling region ①,

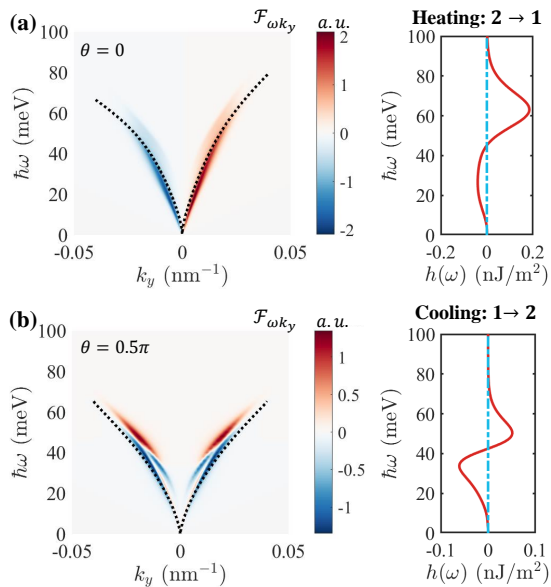


FIG. 2. (a) Left: color plot for energy transmission function ($\mathcal{F}_{\omega k_y}$) as a function of (k_y, ω) with $\theta = 0$. The dot-line is dispersion of surface plasmon polariton at $\omega - k_y$ panel in the Voigt configuration with $k_x = 0$. Right: the corresponding spectrum function $h(\omega)$ with $\Delta T = 0$. (b) Similar as (a) except for $\theta = 0.5\pi$. The dot-line in the left is the dispersion of the surface plasmon polaritons with $k_x = 150k_0$. The drift velocity $v_d = 0.5v_F$ and the gap separation $d = 100\text{nm}$. a.u., arbitrary units

where the active-hot layer 2 can counterintuitively absorb energy from the passive-cold layer 1. Fig. 1(c) reveals the drift velocity v_d dependence of the heating-cooling transition behavior with zero temperature differences: the heating peak is more pronounced at elevated v_d near to zero twist angle; however, the cooling power is unusually robust at large twist angle θ . Further investigation implies that the resulting transition is related to the spectrum match and mismatch caused by the cooperation between the non-reciprocal nature of drifted plasmon polaritons and their topological features near the magic twist angle. Without loss of generality, we fix the temperature difference at zero in the following discussions.

We first discuss the dispersion of the nonreciprocal surface plasmon polaritons in the $\omega - k_y$ panel and its evolution with twist angle. The dispersion for the nonreciprocal surface plasmon polaritons in the cavity formed by the passive- and active-graphene metasurface can be obtained as the singularity of the Fabry-Perot-like denominator matrix:

$$\text{Tr} \left(\mathbf{I} - \mathbf{R}_1 \mathbf{R}_2 e^{-2|k_z|d} \right) = 0, \quad (7)$$

The symmetric breaking in the surface plasmon polariton dispersion ($\omega(k_y) \neq \omega(-k_y)$) emerges at $\theta = 0$ as shown in Fig. 2(a): such nonreciprocal effects are caused by the nonequilibrium drift and increase with the velocity v_d . The roles of such nonreciprocal behavior in the radiative energy transfer are illustrated in terms of the color plot of the k_x -integrated energy transmission function $\mathcal{F}_{\omega k_y}$ which maintains a good

agreement with the dispersion and presents the asymmetric distributions of the cooling (absorbing energy from layer 1 to 2) and heating (transferring energy from layer 2 to 1) modes in the negative and positive k_y , respectively. The direction of net energy flux depends on the competition between these cooling and heating modes. Stating from the low frequency region at the corresponding spectrum function $h(\omega)$ at $\theta = 0$, the cooling modes are dominated channels at $0 < \omega < 45\text{meV}$, where the nonreciprocal effects are not noticeable. With the increased frequency, the heating modes become the dominant channels due to the increased nonreciprocal effects. This enables a positive net energy flux at $\theta = 0$.

However, the competitive situation between the cooling and heating modes can be reversed by rotating the active layer to large angles. Fig. 2(b) shows the recovered symmetric dispersion of the surface plasmon polaritons in $\omega - k_y$ panel with fixed $k_x = 150k_0$ and we can observe the negative net energy flux at $\theta = 0.5\pi$. To understand this, we show a similar symmetric recovery of the k_x -integrated energy transmission function $\mathcal{F}_{\omega k_y}$. The envelope curve of $\mathcal{F}_{\omega k_y}$ also maintains good agreement with the dispersion line, but the distributions of the cooling and heating modes in the $\omega - k_y$ panel are different from those shown in Fig. 2(a): two bands for heating modes in the high frequency region and four bands for cooling modes in the low frequency region, which is analogous to the band splitting effects in electronic band structures. Quantitatively, the extreme anisotropic nature of the bottom passive layer leads to different drag coefficients at different twist angles via near-field coupling to the drifted Dirac electrons in the top active layer, resulting in a redistribution of the cooling and heating modes in momentum k -space. The corresponding spectrum function $h(\omega)$ shows that compared with the spectrum function in Fig. 2(a), the peak for higher-frequency heating modes decreases rapidly but the peak for lower-frequency cooling modes increases at $\theta = 0.5\pi$. Therefore, the interplay of the nonreciprocal and anisotropic Fizeau drag effects gives rise to a negative net energy flux after twisting the active layer at large twist angles.

Twist-induced topological transition in nonreciprocal isofrequency spectrum.— We then study the θ -dependence of the spectrum function $h(\omega)$ and energy transmission function $\mathcal{F}(\omega, k_x, k_y)$ at resonant frequencies of cooling and heating modes. The color plot of $h(\omega)$ is divided into several parts with different topological features at Fig. 3(a). The circled numbers in Fig. 3(a-b) correspond to resonant frequency regions in $\theta - \omega$ phase space and spectrum functions, at $\theta = 0, 0.04\pi, 0.2\pi, 0.48\pi$, respectively. We can find that the resonant heating and cooling modes both have blue shift in the regime with twist angle $0 < \theta < 0.1\pi$ and red shift in the regime with twist angle $0.2\pi < \theta < 0.5\pi$. Note that when $0.1\pi < \theta < 0.2\pi$, the resonant peaks of both modes are significantly reduced, but the reduction of heating modes is severer than that of cooling modes due to different topological transitions. We use the number of anti-crossing points (N_{ACP}) of the dispersion lines of each isolated layer to describe the topological quantity[9]. The dispersion lines of sur-

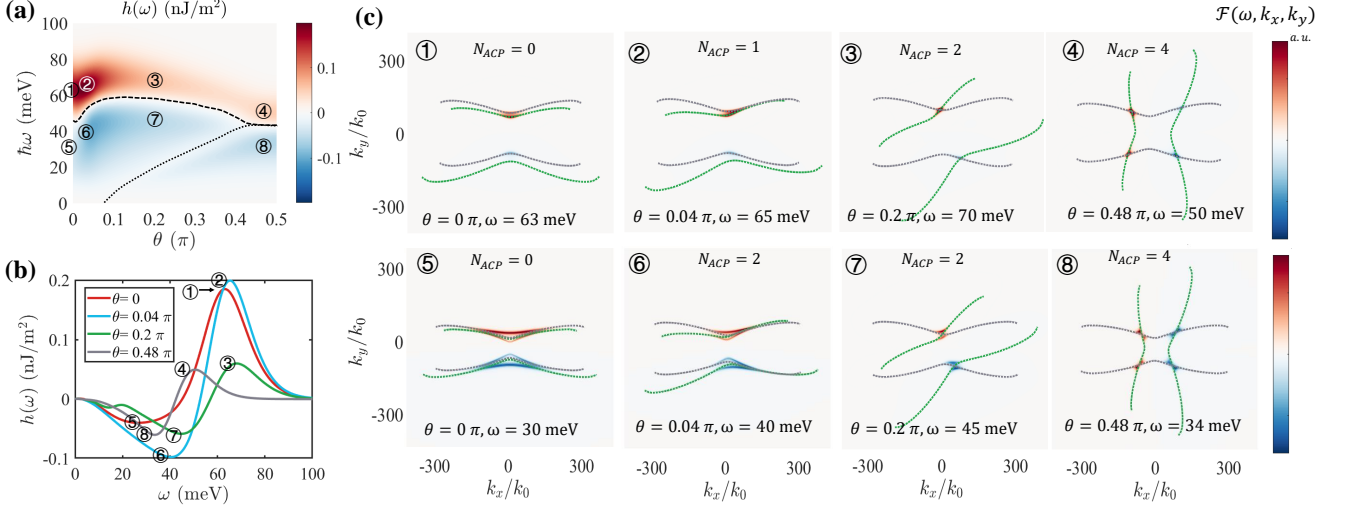


FIG. 3. (a) Color plot for spectrum function $h(\omega)$ as a function of (θ, ω) : the transition line between heating and cooling modes (dashed line), the transition line between cooling modes with different topological features (dotted line), the transition angles for the creation and destruction of different topological polaritons (dash-dotted line). ①-④ are the resonant frequency regions for heating peaks at $\theta = 0, 0.04\pi, 0.2\pi, 0.48\pi$ and ⑤-⑧ are similar regions for cooling peaks. (b) Spectrum function at $\theta = 0, 0.04\pi, 0.2\pi, 0.48\pi$. (c) Energy transmission function $\mathcal{F}(\omega, k_x, k_y)$ at different resonant frequency regions. The grey(green)-dotted lines are the dispersion lines of surface plasmon polaritons in single passive(active) layer. The gap separation d is 100nm and temperature difference is set as zero. a.u., arbitrary units

face plasmon polaritons supported by a single graphene metasurface can be calculated by the poles of the reflection coefficient matrix:

$$(2c\epsilon_0 k_z/k_0 + \sigma_{yy}^{\text{eff}})(2c\epsilon_0 k_0/k_z + \sigma_{xx}^{\text{eff}}) - \sigma_{xy}^{\text{eff}}\sigma_{yx}^{\text{eff}} = 0, \quad (8)$$

where ϵ_0 is the permittivity of vacuum.

Fig. 3(c) shows that the energy transmission functions with heating and cooling bands (represented by the red and blue regions) maintain consistency with the dispersion line of the single graphene metasurface. However, they exhibit different topological transitions, with heating modes following $N_{ACP} = 0 \rightarrow 1 \rightarrow 2 \rightarrow 4$ and cooling modes following $N_{ACP} = 0 \rightarrow 2 \rightarrow 4$, as the twist angle θ increases. At small twist angles, heating and cooling modes take different topological transitions (i.e., $N_{ACP} = 0 \rightarrow 1 \rightarrow 2$ vs $N_{ACP} = 0 \rightarrow 2$ from $\theta = 0$ to $\theta = 0.2\pi$), while demonstrating similar topological transitions at large twist angles (i.e., $N_{ACP} = 2 \rightarrow 4$ from $\theta = 0.2\pi$ to $\theta = 0.4\pi$). Qualitatively, the sign of the spectrum will depend on the topological structure and photon density of states near the N_{ACP} point in k -space. At $\theta = 0$, N_{ACP} equals zero due to the drift-induced nonreciprocal effects (①⑤ in Fig. 3(c)). Energy transfer channels can still be constructed via the scattering processes, but significant mismatch of heating or cooling bands in the high frequency heating modes is observed. As θ increases, the heating bands of heating modes form one nearly degenerate band in the $k_x - k_y$ space, while the cooling bands of heating modes remain large mismatch. Due to the large drift-induced mismatch of high frequency heating modes, this only results in a slight enhancement of the heating peak in the spectrum function (Fig. 3(b)) when $N_{ACP} = 0 \rightarrow 1$. In contrast, the

competition mechanism between heating and cooling bands of cooling modes greatly enhances the contributions of cooling modes. The cooling band of cooling modes with larger radius of curvature in high- k region constructs more channels for energy transfer when $N_{ACP} = 0 \rightarrow 2$. We concluded that such manipulation of thermal-photon carrier density is related to the drift-induced non-reciprocity and twist-induced topological transitions. As the twist angle continues to increase, the flat degenerate bands split and undergo a hyperbolic-elliptic transition, similar to the photonic topological transition in ref[9]. However, all bands of heating and cooling modes undergo a similar topological transition ($N_{ACP} = 2 \rightarrow 4$) at large twist angles, resulting in a saturated heat flux that no longer changes dramatically under further twisting.

Abnormal distance effect at large twist angle.— Another feature in Fig. 3(c) is that the heating modes exist in the interval with higher k value. Such heating modes take a greater attenuation coefficient in the vertical direction of plane compared with the cooling modes, which can lead to an abnormal distance effect. To verify these, we show the ratio between energy flux and blackbody limit versus the gap separation d at $\theta = 0.5\pi$ and 0 in Fig. 4 (for convenience, we set a large-scale temperature difference for blackbody limit, i.e., $T_{BB} = 300\text{K}$). The interval of gap separation is set as 30-100 nm to ensure the validity of effective medium theory applying on the metasurface of graphene strips. We find that there is nonmonotonic distance dependence at $\theta = 0.5\pi$ (red line in Fig. 4) and the energy flux can change the direction with gap separation d increasing. Similar phenomena are discussed in [25] by applying a large magnetic field in magneto-optic media, while here we take a rotation for the nonequilibrium

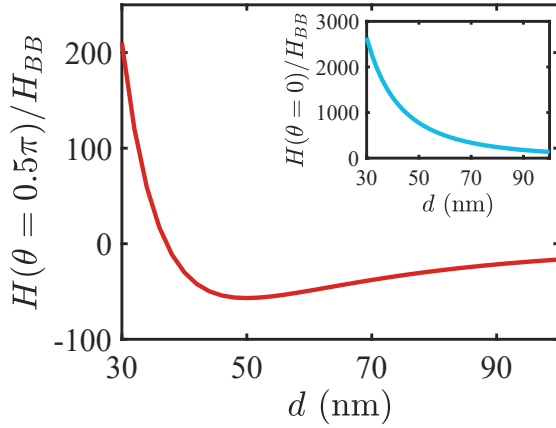


FIG. 4. The ratio between the energy flux H and H_{BB} as a function of gap separation d with $\theta = 0.5\pi$. The temperature difference $\Delta T = 0$ with $T_1 = 300$ K. $H_{BB} = \sigma T_{BB}^4$ is the radiosity of a blackbody at room temperature $T_{BB} = T_1$ and σ is the Stefan-Boltzmann constant. The inset shows the ratio between energy flux with $\theta = 0$ and H_{BB} versus gap separation d .

active graphene metasurface. This is the predictable result of the interplay between nonreciprocal effects and photonic topological transitions: the heating mode with a larger attenuation coefficient will play the dominant role with a smaller gap separation. Notably, our calculations do not violate the second law of thermodynamics: the anomalous energy flow of the inverse temperature gradient can exist in the case of non-equilibrium drift.

In conclusion, we have studied the near-field energy transfer between magic-angle twisted graphene metasurfaces with drifted Dirac electrons. Our findings make a clear case that the current-driven graphene metasurfaces can possess a heating-cooling transition with a rotation regulation. Such behaviour is related to the nonreciprocal photon occupation number from the active graphene metasurface and hyperbolic anisotropy nature from the passive graphene metasurface. Under rotation regulation, the band splitting and degeneracy are observed at resonant frequencies. We therefore conclude that two types of photonic topological transitions exist for heating and cooling modes at a kind of thermal magic angle, arising from the interplay between nonreciprocal and non-local properties of graphene metasurface. The calculations further reveal the unintuitive distance dependence of radiative energy flux under large twist angles. That is, the drifted and twisted near-field radiation becomes thermal insulating when increasing to a critical distance and subsequently reverses the radiative energy flux to anomalously increase the cooling power as increasing distance further. Our work establishes a clear connection between microscopic photonic topological transition and macroscopic heating-cooling transition, which can pave a new way for nanoscale energy transport and thermal managements with nonreciprocity.

This work is supported by the National Natural Science

Foundation of China (No. 11935010), the Shanghai Science and Technology Committee (Grants No. 23ZR1481200), and the Opening Project of Shanghai Key Laboratory of Special Artificial Microstructure Materials and Technology.

* Corresponding Email: jiebin.peng@gdut.edu.cn

† Corresponding Email: xonics@tongji.edu.cn

- [1] Biswajeet Guha, Clayton Otey, Carl B. Poitras, Shanhui Fan, and Michal Lipson, "Near-field radiative cooling of nanostructures," *Nano Letters* **12**, 4546 (2012).
- [2] Yao Zhai, Yaoguang Ma, Sabrina N. David, Dongliang Zhao, Runnan Lou, Gang Tan, Ronggui Yang, and Xiaobo Yin, "Scalable-manufactured randomized glass-polymer hybrid metamaterial for daytime radiative cooling," *Science* **355**, 1062 (2017).
- [3] Riccardo Messina and Philippe Ben-Abdallah, "Graphene-based photovoltaic cells for near-field thermal energy conversion," *Scientific Reports* **3**, 1383 (2013).
- [4] Andrej Lenert, David M. Bierman, Youngsuk Nam, Walker R. Chan, Ivan Celanović, Marin Soljačić, and Evelyn N. Wang, "A nanophotonic solar thermophotovoltaic device," *Nature Nanotechnology* **9**, 126 (2014).
- [5] Achim Kittel, Wolfgang Müller-Hirsch, Jürgen Parisi, Svend-Age Biehs, Daniel Reddig, and Martin Holthaus, "Near-field heat transfer in a scanning thermal microscope," *Phys. Rev. Lett.* **95**, 224301 (2005).
- [6] Yuan Cao, Valla Fatemi, Shiang Fang, Kenji Watanabe, Takashi Taniguchi, Efthimios Kaxiras, and Pablo Jarillo-Herrero, "Unconventional superconductivity in magic-angle graphene superlattices," *Nature* **556**, 43 (2018).
- [7] S. S. Sunku, G. X. Ni, B. Y. Jiang, H. Yoo, A. Sternbach, A. S. McLeod, T. Stauber, L. Xiong, T. Taniguchi, K. Watanabe, P. Kim, M. M. Fogler, and D. N. Basov, "Photonic crystals for nano-light in moiré graphene superlattices," *Science* **362**, 1153 (2018).
- [8] S Dai, Q Ma, M K Liu, T Andersen, Z Fei, M D Goldflam, M Wagner, K Watanabe, T Taniguchi, M Thiemens, F Keilmann, G C A M Janssen, S-E. Zhu, P Jarillo-Herrero, M M Fogler, and D N Basov, "Graphene on hexagonal boron nitride as a tunable hyperbolic metamaterial," *Nature Nanotechnology* **10**, 682 (2015).
- [9] Guangwei Hu, Alex Krasnok, Yarden Mazon, Cheng-Wei Qiu, and Andrea Alù, "Moiré hyperbolic metasurfaces," *Nano Letters* **20**, 3217 (2020).
- [10] LuoJun Du, Maciej R. Molas, Zhiheng Huang, Guangyu Zhang, Feng Wang, and Zhipei Sun, "Moiré photonics and optoelectronics," *Science* **379**, eadg0014 (2023).
- [11] Ivan Latella and Philippe Ben-Abdallah, "Giant thermal magnetoresistance in plasmonic structures," *Phys. Rev. Lett.* **118**, 173902 (2017).
- [12] Ricardo M. Abraham Ekeröth, Philippe Ben-Abdallah, Juan Carlos Cuevas, and Antonio García-Martín, "Anisotropic thermal magnetoresistance for an active control of radiative heat transfer," *ACS Photonics* **5**, 705 (2018).
- [13] Cheng Guo, Bo Zhao, Danhong Huang, and Shanhui Fan, "Radiative thermal router based on tunable magnetic Weyl semimetals," *ACS Photonics* **7**, 3257 (2020).
- [14] Mingjian He, Hong Qi, Yatao Ren, Yijun Zhao, and Mauro Antezza, "Active control of near-field radiative heat transfer by a graphene-gratings coating-twisting method," *Opt. Lett.* **45**,

- 2914 (2020).
- [15] Gaomin Tang, Jun Chen, and Lei Zhang, “Twist-induced control of near-field heat radiation between magnetic weyl semimetals,” *ACS Photonics* **8**, 443 (2021).
- [16] Jiebin Peng, Gaomin Tang, Luqin Wang, Rair Macêdo, Hong Chen, and Jie Ren, “Twist-induced near-field thermal switch using nonreciprocal surface magnon-polaritons,” *ACS Photonics* **8**, 2183 (2021).
- [17] Cheng-Long Zhou, Xiao-Hu Wu, Yong Zhang, Hong-Liang Yi, and Mauro Antezza, “Polariton topological transition effects on radiative heat transfer,” *Phys. Rev. B* **103**, 155404 (2021).
- [18] Rongqian Wang, Jincheng Lu, Xiaohu Wu, Jiebin Peng, and Jian-Hua Jiang, “Tuning topological transitions in twisted thermophotovoltaic systems,” *arXiv:2205.07666*, *Phys. Rev. Applied*, accepted (2023).
- [19] Siddharth Buddhiraju, Wei Li, and Shanhui Fan, “Photonic refrigeration from time-modulated thermal emission,” *Phys. Rev. Lett.* **124**, 077402 (2020).
- [20] Renwen Yu and Shanhui Fan, “Manipulating coherence of near-field thermal radiation in time-modulated systems,” *Phys. Rev. Lett.* **130**, 096902 (2023).
- [21] Juan R. Deop-Ruano and Alejandro Manjavacas, “Control of the radiative heat transfer in a pair of rotating nanostructures,” *Phys. Rev. Lett.* **130**, 133605 (2023).
- [22] Charles H. Henry and Rudolf F. Kazarinov, “Quantum noise in photonics,” *Rev. Mod. Phys.* **68**, 801 (1996).
- [23] Kaifeng Chen, Parthiban Santhanam, Sunil Sandhu, Linxiao Zhu, and Shanhui Fan, “Heat-flux control and solid-state cooling by regulating chemical potential of photons in near-field electromagnetic heat transfer,” *Phys. Rev. B* **91**, 134301 (2015).
- [24] Linxiao Zhu, Anthony Fiorino, Dakotah Thompson, Rohith Mittapally, Edgar Meyhofer, and Pramod Reddy, “Near-field photonic cooling through control of the chemical potential of photons,” *Nature* **566**, 239 (2019).
- [25] Gaomin Tang, Lei Zhang, Yong Zhang, Jun Chen, and C. T. Chan, “Near-field energy transfer between graphene and magneto-optic media,” *Phys. Rev. Lett.* **127**, 247401 (2021).
- [26] Tiago A. Morgado and Mário G. Silveirinha, “Negative Landau damping in bilayer graphene,” *Phys. Rev. Lett.* **119**, 133901 (2017).
- [27] Y. Dong, L. Xiong, I. Y. Phinney, Z. Sun, R. Jing, A. S. McLeod, S. Zhang, S. Liu, F. L. Ruta, H. Gao, Z. Dong, R. Pan, J. H. Edgar, P. Jarillo-Herrero, L. S. Levitov, A. J. Millis, M. M. Fogler, D. A. Bandurin, and D. N. Basov, “Fizeau drag in graphene plasmonics,” *Nature* **594**, 513 (2021).
- [28] Wenyu Zhao, Sihan Zhao, Hongyuan Li, Sheng Wang, Shaoxin Wang, M. Iqbal Bakti Utama, Salman Kahn, Yue Jiang, Xiao Xiao, SeokJae Yoo, Kenji Watanabe, Takashi Taniguchi, Alex Zettl, and Feng Wang, “Efficient Fizeau drag from Dirac electrons in monolayer graphene,” *Nature* **594**, 517 (2021).
- [29] D. Polder and M. Van Hove, “Theory of radiative heat transfer between closely spaced bodies,” *Phys. Rev. B* **4**, 3303 (1971).
- [30] A. I. Volokitin and B. N. J. Persson, “Near-field radiative heat transfer and noncontact friction,” *Rev. Mod. Phys.* **79**, 1291 (2007).
- [31] A. I. Volokitin and B. N. J. Persson, “Theory of the interaction forces and the radiative heat transfer between moving bodies,” *Phys. Rev. B* **78**, 155437 (2008).
- [32] A. I. Volokitin and B. N. J. Persson, “Quantum friction,” *Phys. Rev. Lett.* **106**, 094502 (2011).
- [33] J. Sebastian Gomez-Diaz, Mykhailo Tymchenko, and Andrea Alù, “Hyperbolic plasmons and topological transitions over uniaxial metasurfaces,” *Phys. Rev. Lett.* **114**, 233901 (2015).
- [34] Giampiero Lovat, George W. Hanson, Rodolfo Araneo, and Paolo Burghignoli, “Semiclassical spatially dispersive intraband conductivity tensor and quantum capacitance of graphene,” *Phys. Rev. B* **87**, 115429 (2013).
- [35] D. Correas-Serrano, J. S. Gomez-Diaz, M. Tymchenko, and A. Alù, “Nonlocal response of hyperbolic metasurfaces,” *Opt. Express* **23**, 29434 (2015).